The Journal of Neuroscience, February 15, 2000, *20*(4):1589–1596

Estrogen Selectively Regulates Spine Density within the Dendritic Arbor of Rat Ventromedial Hypothalamic Neurons

Lyngine H. Calizo[1] and Loretta M. Flanagan-Cato[2]

[1]*Institute of Neurological Sciences and* [2]*Department of Psychology, University of Pennsylvania, Philadelphia, Pennsylvania 19104-6074*

Estrogen acts in the hypothalamic ventromedial nucleus (VMH) to promote female sexual behavior. One potential mechanism through which estrogen may facilitate this behavior is by reconfiguring synaptic connections within the VMH. Estrogen treatment increases the number of synapses and dendritic spines in the VMH, but how this remodeling occurs within the context of the local, behaviorally relevant microcircuitry is unknown. The goal of this study was to localize estrogen-induced changes in spine density within the VMH and relate these to dendritic morphology and the presence of nuclear estrogen receptor. The hypothalami from ovariectomized rats, treated with either vehicle or estradiol, were lightly fixed, and VMH neurons were iontophoretically filled with Lucifer yellow. Confocal microscopy was used to examine neuronal morphology. Estrogen treatment increased dendritic spine density by 48% in the ventrolateral VMH but had no effect on spine density in the dorsal VMH. The primary dendrites of VMH neurons were differentially affected by estrogen. Estrogen treatment increased spine density twofold on the short primary dendrites but did not affect spine density on long primary dendrites. Immunocytochemical staining showed that none of the filled neurons expressed estrogen receptor-α. Thus, although the effect of estrogen on spine density is localized to a VMH subdivision where estrogen receptor is expressed, estrogen treatment induces spines on neurons that lack estrogen receptor. Taken together, our results suggest that the effect of estrogen on ventrolateral VMH spines is selective within the dendritic arbor of a neuron and may be mediated by an indirect, possibly transynaptic, mechanism.

Key words: dendritic spines; estrogen; female sexual behavior; lordosis; Lucifer yellow cell filling; VMH

A major goal of behavioral neuroscience is to elucidate the neural basis of motivated behaviors. Female rat sexual behavior has become a valuable model system, in part because the macrocircuitry and hormonal influences are well described (Pfaff et al., 1994). The actions of estrogen in the ventromedial nucleus of the hypothalamus (VMH) are crucial to the promotion of this behavior, as demonstrated by lesion, local infusion, and electrical stimulation experiments (Mathews and Edwards, 1977a,b; Pfaff and Sakuma, 1979a,b; Davis et al., 1982; Pleim et al., 1989). Additionally, receptor autoradiography, immunocytochemistry, and *in situ* hybridization have demonstrated the presence of estrogen receptors in the VMH (Pfaff and Keiner, 1973; Simerly et al., 1990; DonCarlos et al., 1991). Moreover, transneuronal tracing studies have confirmed the serial connectivity of the VMH to the lumbar epaxial muscles that execute the stereotypic female reproductive posture, lordosis (Daniels et al., 1999). Nevertheless, key questions remain about the microcircuitry within the VMH and how estrogen may alter neural connectivity to control the expression of this behavior.

Previous Golgi studies have described the morphology of VMH neurons, which have two to three long, unramified dendrites that extend into the neuropil surrounding the VMH (Szentagothai et al., 1968; Millhouse, 1973b, 1979). VMH dendrites also possess spines (Szentagothai et al., 1968; Millhouse, 1973b, 1979), small protrusions that form specialized sites of synaptic contact (Harris and Kater, 1994). Recent Golgi impregnation studies have suggested that spine density is plastic in a manner that correlates with reproductive behavior. In particular, the density of dendritic spines on VMH neurons fluctuates during the estrous cycle, with an increased density occurring on proestrus compared with diestrus (Frankfurt et al., 1990). In ovariectomized rats, VMH spine density increased twofold after estradiol treatment (Frankfurt et al., 1990). Thus, modulation of spine density in the VMH may be one component of the neural plasticity induced by estrogen to cause the cyclic changes in reproductive behavior.

Unfortunately, Golgi analysis of VMH neurons has not revealed a topographical neuronal organization or morphologically distinct cell types, as has been described in structures like the cerebellum, hippocampus, and neocortex. Consequently, it has not been possible to make functional inferences about VMH neurons based on their relative location or neuronal morphology. Furthermore, the Golgi technique does not allow the concomitant assessment of neurochemical features, such as the expression of receptors and neuropeptides. To better define the microcircuitry of the VMH in the present study, Lucifer yellow cell filling was performed. This technique provided excellent morphological detail. In addition, this approach was compatible with subsequent immunostaining for the estrogen receptor. The present results suggest that the effects of estrogen on spine density are regionally specific and dendrite specific and are not mediated by a direct action of estrogen.

Received Aug. 3, 1999; revised Nov. 19, 1999; accepted Nov. 29, 1999.

L.M.F.-C. is supported by National Institutes of Health Grants MH54712, MH43787, and DK52018. We thank Dr. D. Perkel for generously making his equipment and expertise available to us. We also thank Dr. R. Balice-Gordon, Dr. A. Christie, S. Benton, and J. Cardin for their technical advice, and Drs. D. Perkel and R. Balice-Gordon for their comments on an earlier version of this manuscript.

Correspondence should be addressed to Lyngine H. Calizo, Department of Neuroscience, University of Pennsylvania, 215 Stemmler Hall, 36th and Hamilton Walk, Philadelphia, PA 19104-6074.E-mail: lcalizo@mail.med.upenn.edu.

Copyright © 2000 Society for Neuroscience 0270-6474/00/201589-08$15.00/0

These results were presented in preliminary form at the Society for Behavioral Neuroendocrinology, 1999 (Charlottesville, VA).

MATERIALS AND METHODS

Animals and hormone treatment. Adult female Sprague Dawley rats were housed in plastic tubs with standard bedding and with food and water continuously available. The temperature of the colony was maintained at 22°C with a 12 hr reverse light/dark cycle. Animals were allowed at least 1 week to acclimate to the colony, then ovariectomies were performed during anesthesia using aseptic surgical procedures. After a recovery period of at least 1 week, hormone treatments began, consisting of subcutaneous injections of vehicle ($n = 4$ animals; sesame oil) or estradiol benzoate (EB) ($n = 5$ animals; 10 μg in 100 μl sesame oil) for 2 consecutive days. Body weight during and after hormone treatment, as well as uterine size at the time of perfusion, were monitored to validate the effectiveness of the EB injections. All EB injections were considered effective, based on decreased body weight and increased uterine size compared with vehicle-treated controls.

Perfusion and cell filling. Animals were processed in sets of three. All sets of animals were processed in close succession, and each set included both treatment groups. Thus, the histological manipulations for all animals were comparable.

Forty-eight hours after the second hormone injection, animals were anesthetized with ketamine/xylazine (20 and 80 mg/kg, respectively) and perfused transcardially with 100 ml saline followed by 200 ml 4% paraformaldehyde (purified prill; Electron Microscopy Sciences, Fort Washington, PA). The brains were isolated, and the diencephalon blocks were post-fixed in paraformaldehyde for 3 hr at 4°C. Coronal sections were cut on a vibratome at a thickness of 150 μm in 0.1 M phosphate buffer. The sections were stored in 0.1 M phosphate buffer at 4°C until cell filling, which occurred within 1–3 d after fixation.

For intracellular injections, sections were placed in 0.1 M phosphate buffer on a modified stage of a Leica fluorescent microscope. The sections were viewed using differential interference contrast (DIC) optics, and the stage was positioned so that the VMH could be visualized under a 10× long working distance objective. Intracellular electrodes were constructed from pulled borosilicate glass capillary tubes (1.0 mm outer diameter/0.58 mm inner diameter; World Precision Instruments, Sarasota, FL), with the tips broken to a diameter of ~1 μm. These micropipettes then were backfilled with 4% Lucifer yellow (dilithium salt; Sigma, St. Louis, MO) dissolved in distilled water. The electrode was advanced toward the section with a microdrive mounted on a micromanipulator. Individual cells in the VMH were visualized at 40× magnification under DIC optics and impaled with the electrode. Impalement occurred without intentional bias for any particular size or shape of cell. The cell then was injected iontophoretically over a 10 min period using −30 nA current. The infusion of Lucifer yellow into a cell was observed with fluorescence, and proper impalement was confirmed by rapid infusion of Lucifer yellow into a cell, revealing sharp, well defined borders. An average of two cells were filled per section, five to six sections per animal, which produced 10–12 filled cells per rat. For analysis, these sections were mounted onto glass slides and coverslipped using a mounting media that consisted of glycerol (80%) and 20 mM sodium carbonate (20%). Coverslips were sealed with nail polish.

Morphological analysis. Confocal microscopy and analysis of neuronal morphology were performed blind, and the code was not broken until the data collection was complete. From the 10–12 filled cells per animal, a subset from each animal was chosen for confocal microscopy based on the quality of the fill and likely localization in the VMH (6–7 cells per animal, total = 55 cells). Cells were visualized with a confocal laser scanning microscope (Leica TCS 4D System, Leica, Deerfield, IL) using a 100×, 1.4 NA oil-immersion objective. A single low-power scan (10×) was made of each filled neuron, followed by a high-power scan (100×) consisting of 9–120 serial, optical sections (0.3–0.5 μm thickness). The total number of optical sections taken during the high-power scan depended on the length of the dendrite and the depth that it traveled through the section, because more optical sections were needed to scan longer, deeper extending dendrites. Dendritic spines were counted from individual optical serial sections using NIH software (Image 1.62) on a Macintosh G3. A confocal projection of overlaid optical sections was not used for spine counting because such images obscured a large number of spines above or below the dendrite. In contrast, by viewing the dendrite through a succession of individual optical serial sections, a spine obscured by the dendrite in one optical section became apparent in a successive section(s). However, because no correction was made for spines situated in planes hidden by the dendrite, spine density measurements made by this method potentially underestimate the density of dendritic spines.

The number of spines on each dendritic segment was counted three times, and the mean was used in the final analysis. To verify experimenter reliability, spine counts were repeated on one-third of the animals on two separate occasions, with previous spine counts concealed from the experimenter. Initial spine counts were highly correlated with the two subsequent counts ($p < 0.0001$, $r = 0.99$).

Other measurements included soma size, cell shape, dendritic length, and number of primary dendrites and branch points. To establish the location of a neuron within the VMH, the rostrocaudal position was determined from landmarks, including the optic tracts and median eminence. The mediolateral and dorsoventral positions were plotted using the distance of the cell to the ventral surface of the brain and to the proximal border of the third ventricle. These coordinates then were matched against VMH coordinates according to Paxinos and Watson (1986). A cell was considered to be within the ventrolateral subdivision of the VMH if it was within the subdivision borders indicated by Paxinos and Watson (see Fig. 1). Alternatively, in atlas plates that did not indicate a clear division between the ventrolateral and dorsal subdivisions, a cell was considered to be within the ventrolateral subdivision if it was located in the ventral half of the VMH.

Immunocytochemistry. After morphological analysis, sections were carefully removed from the glass slides for immunostaining procedures. After several washes in TBS, pH 7.4, sections were incubated in estrogen receptor-α antisera (1:200, 1D5; Zymed, South San Francisco, CA) in TBS with 0.2% Triton X-100 and 3% normal donkey serum (Jackson ImmunoResearch, West Grove, PA) for 1 hr at room temperature, and then for 72 hr at 4°C. After several washes, sections were incubated in biotinylated donkey anti-mouse antisera (1:1000, Jackson ImmunoResearch) in TBS with 0.2% Triton X-100 and 3% normal donkey serum (Jackson ImmunoResearch) for 4 hr at room temperature. After several washes, sections were incubated in cy5-conjugated streptavidin (1:1000, Jackson ImmunoResearch) in TBS with 0.2% Triton X-100, overnight at 4°C. After final washing, sections were mounted on slides and coverslipped with VectaShield (Vector Laboratories, Burlingame, CA), and coverslips were sealed with nail polish. Cells were imaged with a confocal laser scanning microscope (Leica TCS 4D System, Leica, Deerfield, IL) using a 40×, 1.25 NA oil-immersion objective.

Statistical analysis. Cells included in the final analysis had to meet two criteria. First, the soma had to be located within the VMH, as described above. Fifty-four of the 55 analyzed filled cells met this criterion. Second, the average spine density for each cell had to pass the extreme studentized deviate test for outliers. Fifty-three of the remaining 54 cells met this criteria. For each dendrite, spine density was calculated as the average number of spines per millimeter of dendrite. For each neuron, total spine density was calculated by averaging the spine density for all dendrites. The spine density for each animal, then, was calculated as an average of the total spine density for all its filled neurons. Statistical comparisons were performed by Student's t test (two groups) or ANOVA (multiple groups). When appropriate, *post hoc* analysis was performed using the least significant difference (LSD) test. Circular statistics were used for comparisons of spatial orientation analysis, namely the Rayleigh and the χ^2 test (Batschelet, 1981). Significance was set at $p < 0.05$.

RESULTS

A total of 53 Lucifer yellow-filled neurons in the VMH were included in the final analysis (five to six cells per animal, nine animals). Most of these neurons resided in the ventrolateral VMH (vlVMH, 60%, $n = 31$ cells), with the remaining neurons in the dorsal subdivision (40%, $n = 22$ cells) (Fig. 1). The morphological features of the Lucifer yellow-filled neurons were similar to those previously observed in other studies using Golgi impregnation (Table 1) (Szentagothai et al., 1968; Millhouse, 1973b, 1979). Most neurons were spherical or ovoid with long, relatively straight, sparsely branched, spinous dendrites. On average, there were two primary dendrites per neuron, with approximately one branch point in each dendritic tree. Although most dendrites were straight, some were twisted. In most cases the end of the dendrite was tapered, but in other cases it was rounded. Axons were occasionally observed and appeared as thin, beaded

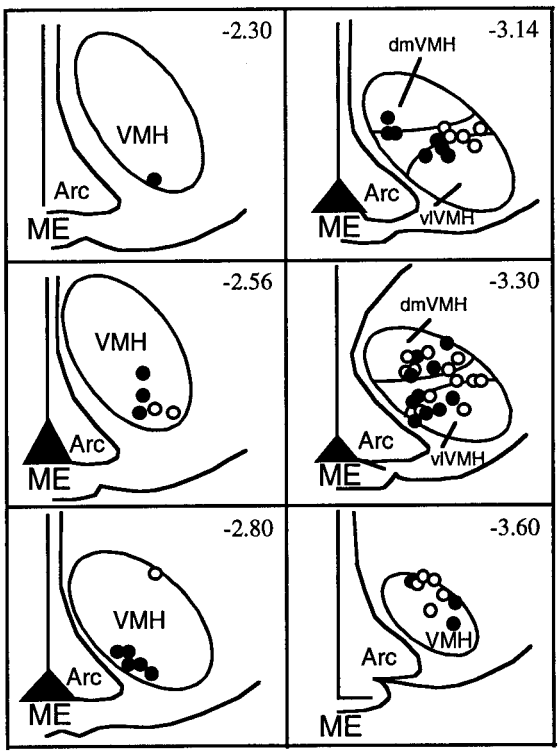

Figure 1. Composite drawings of the locations of Lucifer yellow-filled cells within the VMH from vehicle-treated (○) and EB-treated (●) rats. Cell location was estimated by matching the measured distance of the cell from the ventral surface of the brain and from the third ventricle with coordinates from Paxinos and Watson (1986). *Numbers* to the *right* indicate each section's coordinates posterior from Bregma. *Arc*, Arcuate; *ME*, median eminence; *VMH*, ventromedial hypothalamic nucleus; *dmVMH*, dorsomedial subdivision of the VMH; *vlVMH*, ventrolateral subdivision of the VMH. Drawings are modified tracings based on Paxinos and Watson (1986).

Table 1. Analysis of the morphological features of VMH neurons filled with Lucifer yellow

	Oil (n = 4)	EB (n = 5)
Soma area (μm^2)	107.10 ± 2.07	116.70 ± 10.44
Dendrites/neuron	2.9 ± 0.2	2.8 ± 0.2
Primary dendrites/neuron	2.1 ± 0.1	1.9 ± 0.1
Branch points/neuron	0.8 ± 0.2	0.9 ± 0.2
Dendrite length (μm)	113.50 ± 10.31	111.10 ± 15.08

Cells were filled iontophoretically with Lucifer yellow and visualized using confocal microscopy. Measurements were made on NIH Image 1.62 (mean ± SEM). EB, Estradiol benzoate. These measurements are consistent with previous Golgi studies (see Results and Discussion).

processes. Confocal microscopic imaging of Lucifer yellow-filled neurons provided excellent visualization of dendritic spines.

Estrogen treatment increased the average density of dendritic spines in the vlVMH per neuron per animal by 48% ($p < 0.05$, Student's t test) (Fig. 2). This effect was region-specific, because no effect of estrogen was observed in the dorsal VMH. Examples of dendritic spines for each group are shown in Figure 3.

Subsequent analysis focused on the dendritic arbor of vlVMH neurons. Dendrites of vlVMH neurons were segregated into mutually exclusive categories that differed significantly in their basic characteristics and in their response to estrogen. Dendrites were classified as either long primary (longest primary dendrite),

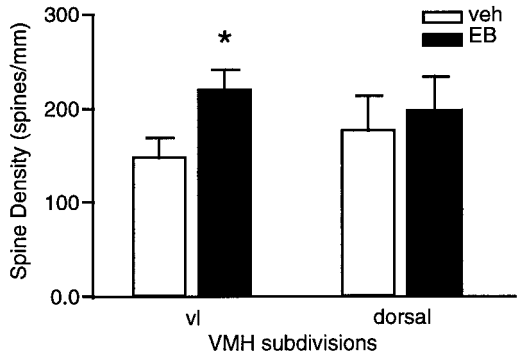

Figure 2. Comparison of dendritic spine density in the ventrolateral VMH and dorsal VMH from vehicle-treated (n = 4) and EB-treated (n = 5) rats (mean ± SEM). EB treatment significantly increases spine density in the ventrolateral but not the dorsal VMH. Spines were counted from confocal movie images, and length was measured using NIH Image 1.62. Spine density values are expressed in number of spines per millimeter dendrite per cell per rat. Ventrolateral VMH: two to five cells/animal, 4–17 dendrites/animal. Dorsal VMH: one to four cells/animal, 2–13 dendrites/animal. *Asterisk* indicates $p < 0.05$, Student's t test. *Veh*, Vehicle; *EB*, estradiol benzoate; *vl*, ventrolateral.

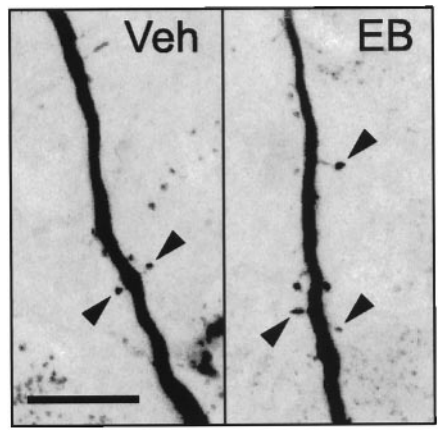

Figure 3. Digital micrographs from a confocal projection of representative dendrite segments from vehicle- and EB-treated rats. Individual serial optical sections were overlaid to create this figure. Actual spine counts were made from individual optical sections rather than an overlaid image as seen here. *Arrows* point to examples of apparent dendritic spines in the overlaid image. Certain spines appeared with more clarity in individual optical sections. Confocal images were converted to gray scale and inverted to a negative image using Adobe Photoshop 4.0. Scale bar, 10 μm. *Veh*, Vehicle; *EB*, estradiol benzoate.

short (non-longest) primary, or secondary. By definition every neuron had only one "long" primary dendrite. vlVMH neurons had an average of 1.0 ± 0.2 short dendrites per neuron (mean ± SEM). On average, the long primary dendrites were fourfold longer than the dendrites in the remaining categories (Fig. 4). Estrogen treatment, however, did not affect the length of any type of dendrite. Thus, the estrogen-induced increase in spine density, described above, could not be explained by a decrease in dendrite length. The long and short primary dendrites also differed in their overall spatial orientations ($p < 0.01$, χ^2 test), which were classified as either dorsolateral, ventrolateral, ventromedial, or dorsomedial. The long primary dendrites were significantly oriented in the ventrolateral direction (vector length = 0.4909, $p < 0.01$, Rayleigh test), whereas short primary dendrites showed no directional preference (Fig. 5). Thus, this classification of primary

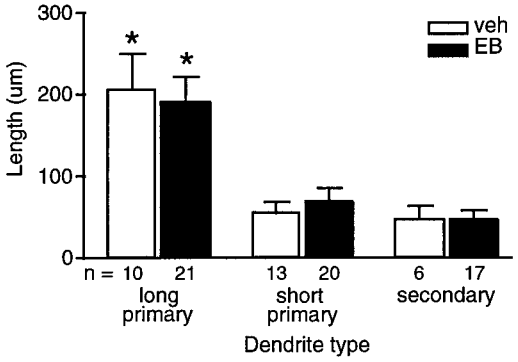

Figure 4. Comparison of the lengths of the long primary, short primary, and secondary ventrolateral VMH dendrites (mean ± SEM, n = number of dendrites). Estrogen treatment did not affect the length of any dendrite type. Dendrite length depended on dendrite class ($F_{(2,80)} = 22.26$, $p < 0.01$, two-way ANOVA). The mean length of the long primary dendrites was significantly different from those of the other dendrite types. Lengths were measured using NIH Image 1.62. *Asterisk* indicates $p < 0.01$ on *post hoc* analysis (LSD). *veh*, Vehicle; *EB*, estradiol benzoate.

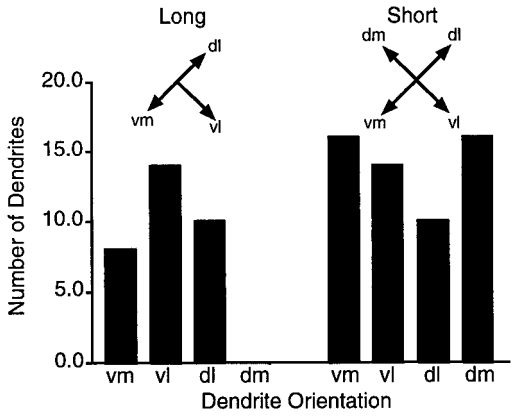

Figure 5. Spatial orientation of long and short primary dendrites of the ventrolateral VMH. Dendrites were classified as projecting in the ventromedial (*vm*), ventrolateral (*vl*), dorsolateral (*dl*), or dorsomedial (*dm*) direction. Long primary dendrites had a significant preference for the ventrolateral direction (χ^2 test and Rayleigh test, $p < 0.05$), whereas short primary dendrites were randomly oriented.

dendrites can be justified based on both length and spatial orientation differences.

Subsequent analysis addressed whether estrogen treatment differentially regulated spine density on the long and short primary dendrites of vlVMH neurons. The effect of estrogen on spine density differed depending on dendrite category ($F_{(1,61)} = 4.20$, $p < 0.05$, two-way ANOVA). Estrogen increased spine density by approximately 2.5-fold on the short primary dendrites ($p < 0.05$, LSD) without affecting spine density on the long primary dendrites (Fig. 6). Estrogen treatment did not alter spine density on the secondary dendrites.

Detection of spine induction on the short, but not the long, primary dendrites would occur if estrogen treatment has differential effects on the two types of dendrites. Alternatively, estrogen might induce spines close to the soma on both types of dendrites. If so, the unaffected distal regions of the long primary dendrites might obscure an effect on these dendrites. To examine this possibility, spines were recounted on 50 μm segments of the primary dendrites. Both proximal (0–50 μm from the soma) and distal (100–150 μm and 150–200 μm from the soma) dendritic

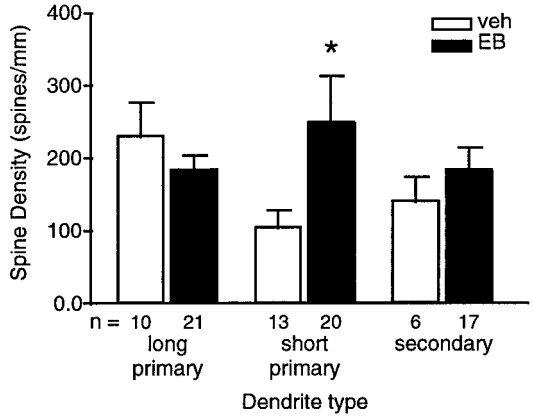

Figure 6. Comparison of spine densities of the long primary, short primary, and secondary dendrites of ventrolateral VMH cells from vehicle- and estrogen-treated rats (mean ± SEM, n = number of dendrites). The effect of estrogen depended on dendrite class ($F_{(1,61)} = 4.20$, $p < 0.05$, two-way ANOVA). Estrogen increased spine density in the short primary dendrites without affecting spine density on the long primary dendrites. *Asterisks* indicates $p < 0.05$ on *post hoc* analysis (LSD). Estrogen treatment did not alter spine density on secondary dendrites. *veh*, Vehicle; *EB*, estradiol benzoate.

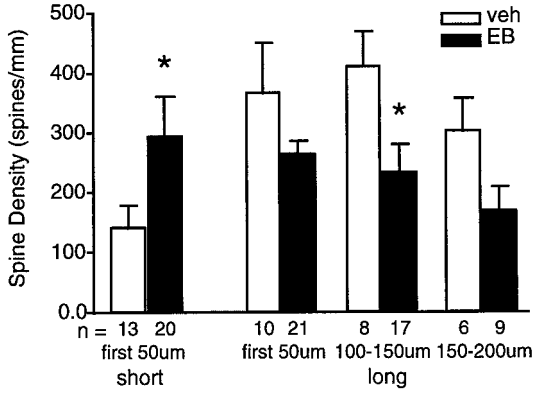

Figure 7. Comparison of spine density on 50 μm dendritic segments of the long and short primary dendrites of ventrolateral VMH neurons from vehicle- and estrogen-treated rats (mean ± SEM, n = number of dendrites). Within the first 50 μm of dendrite, the effect of estrogen on spine density differed between long and short dendrites ($F_{(1,61)} = 5.44$, $p < 0.05$, two-way ANOVA). Estrogen increased spine density on the first 50 μm of the short primary dendrites, but did not affect spine density on the first 50 μm of the long primary dendrites. On the long primary dendrites, the effect of estrogen on spine density did not depend on proximity to soma nor did proximity to soma itself affect spine density. However, overall, estrogen treatment decreased spine density ($F_{(1,67)} = 10.66$, $p < 0.01$, two-way ANOVA). This decrease was significant on dendritic segments 100–150 μm from the soma. *Asterisks* indicate $p < 0.05$ on *post hoc* analysis (LSD). *veh,* Vehicle; *EB*, estradiol benzoate.

segments were analyzed. Within the first 50 μm of dendrite, the effect of estrogen on spine density differed between long and short dendrites ($F_{(1,61)} = 5.44$, $p < 0.05$, two-way ANOVA). Estrogen increased spine density on the first 50 μm of the short primary dendrites ($p < 0.05$, LSD), but did not affect spine density on the first 50 μm of the long primary dendrites (Fig. 7).

By comparing proximal and distal segments, spine density on the long primary dendrites then was assessed for a possible interaction between estrogen treatment and distance from the soma. The corresponding analysis on the distal segments of short dendrites could not be performed because very few dendrites in

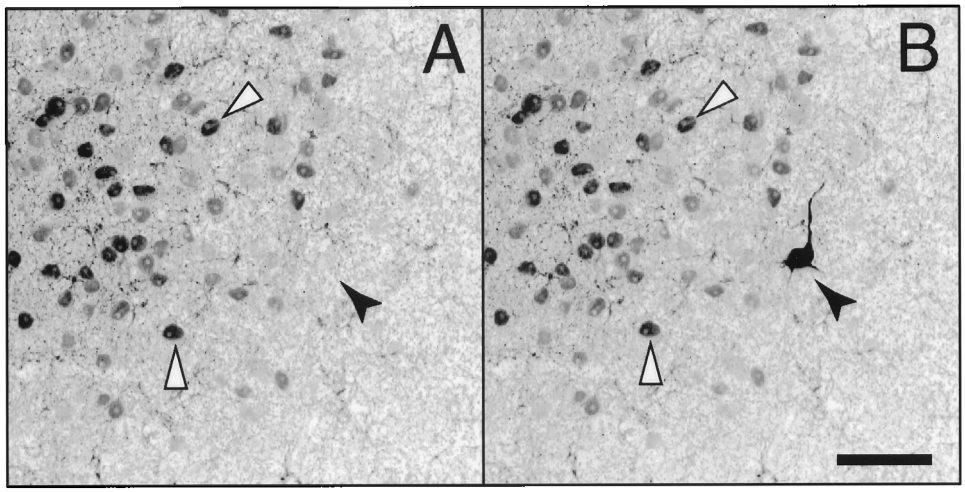

Figure 8. Digital micrographs of representative Lucifer yellow-filled cells and estrogen receptor-containing neurons in the ventrolateral VMH. *A*, Estrogen receptor-α immunoreactive neurons labeled with cy5. *B*, Composite image of cy5-labeled estrogen receptor-α immunoreactive neurons and Lucifer yellow-filled cell. Only a portion of the dendritic arbor of the Lucifer yellow-filled cell is shown. Confocal images were converted to gray scale and inverted to a negative image using Adobe Photoshop 4.0. *White arrowheads* indicate estrogen receptor-α-immunoreactive neurons. *Black arrowhead* indicates (*B*) a Lucifer yellow-filled neuron or (*A*) the location of a Lucifer yellow-filled neuron. Scale bar, 50 μm.

this category extended beyond 100 μm. Proximity to soma itself did not affect spine density significantly on the long primary dendrites. In addition, the effect of estrogen treatment did not depend on proximity to soma. However, estrogen treatment did decrease spine density on the long primary dendrites ($F_{(1,67)} = 10.66, p < 0.01$, two-way ANOVA). This decrease was significant on the dendritic segment 100–150 μm from the soma ($p < 0.05$, LSD) (Fig. 7).

Because vlVMH is abundant in estrogen receptor-containing neurons (Pfaff and Keiner, 1973; Simerly et al., 1990; DonCarlos et al., 1991; Shugrue et al., 1992), it is reasonable to propose that in this brain region estrogen-induced spines may occur on neurons that express estrogen receptor. If so, spine induction may be mediated by a direct, genomic effect of estrogen within the cell. Alternatively, if spine induction occurs in neurons that do not express estrogen receptor, such a direct mechanism would seem unlikely. To elucidate the mechanisms of estrogen-induced spines in the VMH, sections with Lucifer yellow-filled cells in the vlVMH were immunostained with an estrogen receptor-α antibody. Previous studies have demonstrated that immunostaining is compatible with Lucifer yellow cell filling and that Lucifer yellow does not interfere with the immunoreactivity of other antigens (Kawata et al., 1983; Pilowksy et al., 1991). Consistent with earlier studies (Pfaff and Keiner, 1973; Simerly et al., 1990; Shugrue et al., 1992), abundant nuclear staining for the estrogen receptor was visible in the area around the ventrolateral border of the vlVMH. Some of the Lucifer yellow-filled cells were in close proximity to estrogen receptor-containing cells. However, the majority of Lucifer yellow-filled cells in the vlVMH were somewhat medial to the estrogen receptor cluster. All 31 of the Lucifer yellow-filled cells located in the vlVMH were clearly visible after immunostaining and could be easily distinguished from the immunostained cells. Nevertheless, in both groups, none of the Lucifer yellow-filled cells were co-labeled for nuclear estrogen receptor-α (Fig. 8). The Lucifer yellow-filled cells were predominantly located in the medial portion of the vlVMH, whereas the estrogen receptor cluster was visible in the area near the ventrolateral border of the vlVMH. Thus, based on their location, it is not unusual that none of the Lucifer yellow-filled cells were labeled for estrogen receptor-α. The lack of estrogen receptor-α in the Lucifer yellow-filled cells suggests that spine induction within these neurons does not occur through a direct, genomic mechanism. This interpretation allows for a genomic effect on the nearby estrogen receptor-α-containing neurons, which may transynaptically induce spines on cells that do not possess estrogen receptor-α. Such a mechanism has been proposed in the hippocampus (Murphy et al., 1998). Although we document spine density changes on neurons lacking estrogen receptor-α, it remains to be determined whether such changes occur on estrogen receptor-α-positive neurons.

DISCUSSION

The goal of this study was to elucidate the neural elements of the microcircuitry within the VMH that exhibit estrogen-induced neural plasticity. Previous work has shown that estrogen increases dendritic spine density in the VMH (Frankfurt et al., 1990). Our results go beyond these original observations in three important ways. First, within the VMH the induction of spines is subdivision specific. Second, although the dendritic arbors of VMH neurons are simple, anatomical evidence exists for dendrite specialization. This is supported by the finding that estrogen specifically induces spines in short primary vlVMH dendrites. Third, spine induction by estrogen occurs on neurons that, based on immunostaining, do not express nuclear estrogen receptor-α. Each of these findings is discussed in turn.

Initial studies used Golgi impregnation to define the morphology of VMH neurons (Szentagothai et al., 1968; Millhouse, 1973b, 1979). Our results with Lucifer yellow-filled cells revealed morphological features similar to those described, particularly with regard to cell size, dendrite number, and dendrite length (Szentagothai et al., 1968, Frankfurt et al., 1990; Millhouse, 1973b, 1979). Overall, somewhat higher spine density values were obtained with Lucifer yellow cell filling (100–300 spines/mm) than have been detected with Golgi (50–200 spines/mm) (Frankfurt et al., 1990; Frankfurt and McEwen, 1991a). A likely explanation for this discrepancy is that Golgi-impregnated cells were analyzed using camera lucida drawings under light microscopy, whereas the Lucifer yellow-filled cells were visualized using confocal microscopy, which allows the detection of spines that would otherwise be obscured by the dendrite. Overall, these two techniques provide comparable morphological results.

Our observation that estrogen-induced spines are localized to the vlVMH is noteworthy, given the evidence that this subdivision is involved in female sexual behavior. Sexual behavior selectively induces immediate early gene expression in the vlVMH but not the dorsal VMH (Flanagan et al., 1993; Pfaus et al., 1993;

Tetel et al., 1993; Polston and Erskine, 1995). Additionally, estrogen receptor-containing neurons are found specifically in the vlVMH (Pfaff and Keiner, 1973; Simerly et al., 1990; DonCarlos et al., 1991). Moreover, the descending projections of the ventrolateral but not the dorsal VMH target the ventrolateral periaqueductal gray (Canteras et al., 1994), the subdivision thought to be involved in the lordosis posture (Lonstein and Stern, 1998; Daniels et al., 1999). Although the regional specificity of estrogen-induced spines in the VMH implicates them in sexual behavior, it remains to be established whether these spines represent legitimate synapses. Another question about the function of the induced spines is whether they contribute to the priming actions of estrogen for sexual behavior or to the execution of this behavior.

In addition to regional specificity, we also found that the effects of estrogen are spatially organized within the dendritic tree. The simple arborization of VMH dendrites has been described previously (Szentagothai et al., 1968; Millhouse, 1973b, 1979). The present study found differences in the length and direction of the primary dendrites that suggested functional differences. For instance, the short primary dendrites may receive input from local vlVMH neurons. In contrast, long, ventrolaterally oriented dendrites may receive input from the neuropil, which is rich with extrinsic afferents and runs along the lateral edge of the VMH (Millhouse, 1973a). Further evidence for differential innervation of these two dendrite types was provided by the differential effects of estrogen on their spine density. Spine density is differentially regulated based on dendrite-specific afferent input. For instance, in hippocampal cultures, afferent input to specific dendrites alters spine density on those dendrites without generalized effects on the remaining dendrites (Kossel et al., 1997). Thus, short primary dendrites in the vlVMH may receive estrogen-modulated afferent input that is unavailable to the long primary dendrites.

The dendrite specificity of estrogen-induced spines in the VMH may not have been detected in previous studies that analyzed only a single primary dendrite, specifically, the primary dendrite with the "greatest number of spines" (Frankfurt et al., 1990) or the "second longest primary dendrite" (Segarra and McEwen, 1991). Because results of the former study are similar to those of the present study, it is possible that the sample consisted mainly of short dendrites. The second longest primary dendrite of the latter study would be a subset of our short primary dendrites. Thus, the present results replicate previous findings, but our more complete analysis of the dendritic tree has revealed that the effect of estrogen is selective within the dendritic arbor.

In addition to spine induction, we have detected a decrease in spine density on the distal portions of the long primary vlVMH dendrites. This result suggests that differential afferent input occurs along the length of long dendrites such that estrogen selectively alters the strength of inputs within specific segments of the long dendrites. Consequently, the effect of estrogen differs not only between dendrite categories (long vs short), but also within specific segments of the long dendrites. The concomitant spine density increase in short dendrites and decrease in long dendrites may explain why estrogen treatment did not seem to alter the number of axospinous synapses in the estrogen-treated rat vlVMH in previous electron microscopy studies (Nishizuka and Pfaff, 1989; Frankfurt and McEwen, 1991b). In particular, averaging of both dendrite types may have concealed the effect of estrogen on these synapses.

To explore the cellular mechanisms of estrogen-induced spines, we immunostained Lucifer yellow-filled vlVMH cells for estrogen receptor-α. None of the cells in either treatment group expressed nuclear estrogen receptor. This suggests that estrogen did not act through direct, genomic mechanisms within these neurons to increase spine density. Instead, estrogen may act indirectly, altering activity afferent to the filled neurons. Many studies in the telencephalon have shown that the induction and maintenance of dendritic spines depends on afferent input (Annis et al., 1994; Bundman et al., 1994; Kossel et al., 1997; McKinney et al., 1999), particularly through glutamate receptors (Goldowitz et al., 1979; Kossel et al., 1997; McKinney et al., 1999). In fact, estrogen induces spines through a glutamate receptor-dependent mechanism in hippocampal CA1 neurons (Woolley and McEwen, 1994; Murphy and Segal, 1996). The role of glutamate in estrogen-induced vlVMH spines is unclear. However, several lines of circumstantial evidence support this mechanism. First, NMDA and AMPA receptors have been localized to the VMH (Brann and Mahesh, 1994; Meeker et al., 1994; van den Pol et al., 1994, 1995; Mateos et al., 1998). Second, estrogen increases VMH glutamate levels (Mansky and Wuttke, 1983; Frankfurt et al., 1984; Luine et al., 1997). Third, estrogen priming of rat sexual behavior requires glutamatergic receptor activation (Fleischmann et al., 1991). However, because hypothalamic spine induction mechanisms have not been well studied, it seems premature to rule out the contributions of other neurotransmitters (Frankfurt and McEwen, 1991a).

Regardless of the neurotransmitter system involved, the effect of estrogen on cells lacking estrogen receptor suggests that estrogen acts transynaptically, rather than directly, to induce dendritic spines. The key question, then, is whether the afferents that stimulate spine formation are extrinsic or intrinsic to the VMH. Previous anatomical studies have suggested that extrinsic afferents to the vlVMH are found in the neuropil surrounding the VMH (Millhouse, 1973a; Swanson and Hartman, 1975). In sup-

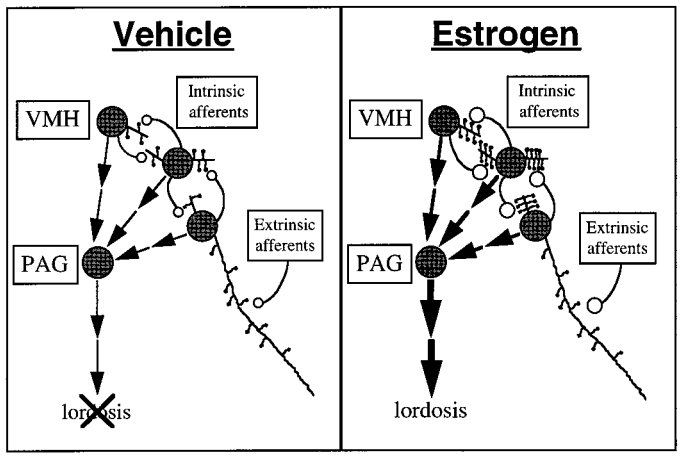

Figure 9. Model of possible mechanisms of spine induction on short primary dendrites in the ventrolateral VMH. The effect of estrogen on cells lacking estrogen receptor suggests that estrogen acts transynaptically, rather than directly, to induce dendritic spines. The afferents that stimulate spine formation may be either extrinsic or intrinsic to the VMH. Extrinsic afferents are mainly found in the neuropil surrounding the VMH. Long primary dendrites extending to the ventrolateral border of the VMH may be innervated by extrinsic afferents in the neuropil. Intrinsic afferents may innervate short primary dendrites. We propose that estrogen affects local intrinsic afferents to increase spine density on short primary dendrites. *Open circles* indicate excitatory synapses; *arrows* indicate direction of information flow through the circuit. *VMH*, Ventromedial nucleus of the hypothalamus; *PAG*, periaqueductal gray.

port of the importance of extrinsic afferents for estrogen-induced neural plasticity, VMH denervation prevented estrogen-induced axodendritic synapse formation (Nishizuka and Pfaff, 1989). The length and ventrolateral orientation of the long dendrites suggest that they are more likely to be innervated by the afferents in the neuropil. It is currently unclear how extrinsic afferent innervation on long dendrites would lead to increased spines on short dendrites. Alternatively, estrogen may increase local afferent activity on the short dendrites, leading to increased spine formation on these same dendrites. This afferent input may be provided by nearby estrogen receptor-containing vlVMH neurons (Fig. 9). The fact that the spine density changes occur in neurons lacking estrogen receptor might be interpreted to suggest that this phenomenon is not related to sexual behavior. However, the location of our filled cells closely matches the effective stimulation sites used in a previous study using electrical stimulation within the VMH to facilitate sexual behavior, i.e., medial to the cluster of estrogen receptor-containing cells (Pfaff and Sakuma, 1979b).

In conclusion, the effects of estrogen on reproductive behavior appear to involve various changes in the synaptic organization of the vlVMH, including dendrite-specific changes in spine density. These results suggest that estrogen differentially modulates the strength of multiple afferents to vlVMH neurons. However, the source of these afferents and the site and mechanism of estrogen action remain as key questions. The fact that this phenomenon occurs in a brain region critical for female sexual behavior suggests that the induced spines may be involved in the priming action of estrogen and/or actual execution of receptive behaviors. The lack of estrogen receptor immunoreactivity in these cells suggests that spine induction is mediated by an indirect mechanism possibly involving afferent stimulation. Future studies are needed to determine (1) the phenotype and function of the neurons that exhibit estrogen-induced spines and (2) whether estrogen receptor-α-containing neurons also exhibit estrogen-induced dendritic spines.

REFERENCES

Annis CM, O'Dowd DK, Robertson RT (1994) Activity-dependent regulation of dendritic spine density on cortical pyramidal neurons in organotypic slice culture. J Neurobiol 25:1483–1493.

Batschelet E (1981) Circular statistics in biology. New York: Academic.

Brann DW, Mahesh VB (1994) Excitatory amino acids: function and significance in reproduction and neuroendocrine regulation. Front Neuroendocrinol 15:3–49.

Bundman MC, Pico RM, Gall CM (1994) Ultrastructural plasticity of the dentate gyrus granule cells following recurrent limbic seizures: increase in somatic spines. Hippocampus 4:601–610.

Canteras NS, Simerly RB, Swanson LW (1994) Organization of projections from the ventromedial nucleus of the hypothalamus: a *Phaseolus vulgaris*-leucoagglutinin study in the rat. J Comp Neurol 348:41–79.

Daniels D, Miselis RR, Flanagan-Cato LM (1999) Central neuronal circuit innervating the lordosis-producing muscles defined by transneuronal transport of pseudorabies virus. J Neurosci 19:2823–2833.

Davis PG, Krieger MS, Barfield RJ, McEwen BS, Pfaff DW (1982) The site of action of intrahypothalamic estrogen implants in feminine sexual behavior: an autoradiographical analysis. Endocrinology 111:1581–1586.

DonCarlos LL, Monroy E, Morrell JI (1991) Distribution of estrogen receptor-immunoreactive cells in the forebrain of the female guinea pig. J Comp Neurol 305:591–612.

Flanagan LM, Pfaus JG, Pfaff DW, McEwen BS (1993) Induction of Fos immunoreactivity in oxytocin neurons after sexual activity in female rats. Neuroendocrinology 58:352–358.

Fleischmann A, Vincent PA, Etgen AM (1991) Effects of noncompetitive NMDA receptor antagonists on reproductive and motor behaviors in female rats. Brain Res 568:138–146.

Frankfurt M, McEwen BS (1991a) 5,7-Dihydroxytryptamine and gonadal steroid manipulation alter spine density in ventromedial hypothalamic neurons. Neuroendocrinology 54:653–657.

Frankfurt M, McEwen BS (1991b) Estrogen increases axodendritic synapses in the VMN of rats after ovariectomy. NeuroReport 2:380–382.

Frankfurt M, Fuchs E, Wuttke W (1984) Sex differences in the γ-aminobutyric acid and glutamate concentrations in discrete rat brain nuclei. Neurosci Lett 50:245–250.

Frankfurt M, Gould E, Woolley CS, McEwen BS (1990) Gonadal steroids modify dendritic spine density in ventromedial hypothalamic neurons: a Golgi study in the adult rat. Neuroendocrinology 51:530–535.

Goldowitz D, Scheff S, Cotman CW (1979) The specificity of reactive synaptogenesis: a comparative study in the adult rat hippocampal formation. Brain Res 170:427–441.

Harris KM, Kater SB (1994) Dendritic spines: cellular specializations imparting both stability and flexibility to synaptic function. Annu Rev Neurosci 17:341–371.

Kawata M, Sano Y, Inenaga K, Yamashita H (1983) Immunohistochemical identification of Lucifer yellow-labeled neurons in the rat supraoptic nucleus. Histochemistry 78:21–26.

Kossel AH, Williams CV, Schweizer M, Kater SB (1997) Afferent innervation influences the development of dendritic branches and spines via both activity-dependent and non-activity-dependent mechanisms. J Neurosci 17:6314–6324.

Lonstein JS, Stern JM (1998) Site and behavioral specificity of periaqueductal gray lesions on postpartum sexual, maternal and aggressive behaviors in rats. Brain Res 804:21–35.

Luine VN, Grattan DR, Selmanoff M (1997) Gonadal hormones alter hypothalamic GABA and glutamate levels. Brain Res 747:165–168.

Mansky T, Wuttke W (1983) Glutamate in hypothalamic and limbic structures of diestrous, proestrous, ovariectomized and ovariectomized estrogen-treated rats. Neurosci Lett 38:51–56.

Mateos JM, Azkue J, Benitez R, Sarria R, Losada J, Conquet F, Ferraguti F, Kuhn R, Knopfel T, Grandes P (1998) Immunocytochemical localization of the mGluR1b metabotropic glutamate receptor in the rat hypothalamus. J Comp Neurol 390:225–233.

Mathews D, Edwards DA (1977a) Involvement of the ventromedial and anterior hypothalamic nuclei in the hormonal induction of receptivity in the female rat. Physiol Behav 19:319–326.

Mathews D, Edwards DA (1977b) The ventromedial nucleus of the hypothalamus and the hormonal arousal of sexual behaviors in the female rat. Horm Behav 8:40–51.

McKinney RA, Capogna M, Durr R, Gahwiler BH, Thompson SM (1999) Miniature synaptic events maintain dendritic spines via AMPA receptor activation. Nat Neurosci 2:44–49.

Meeker RB, Greenwood RS, Hayward JN (1994) Glutamate receptors in the rat hypothalamus and pituitary. Endocrinology 134:621–629.

Millhouse OE (1973a) Certain ventromedial hypothalamic afferents. Brain Res 55:89–105.

Millhouse OE (1973b) The organization of the ventromedial hypothalamic nucleus. Brain Res 55:71–87.

Millhouse OE (1979) A Golgi anatomy of the rodent hypothalamus. In: Handbook of the hypothalamus: anatomy of the hypothalamus (Morgane PJ, Panksepp J, eds), pp 221–265. New York: Marcel Dekker.

Murphy DD, Segal M (1996) Regulation of dendritic spine density in cultured rat hippocampal neurons by steroid hormones. J Neurosci 16:4059–4068.

Murphy DD, Cole NB, Greenberger V, Segal M (1998) Estradiol increases dendritic spine density by reducing GABA neurotransmission in hippocampal neurons. J Neurosci 18:2550–2559.

Nishizuka M, Pfaff DW (1989) Intrinsic synapses in the ventromedial nucleus of the hypothalamus: an ultrastructural study. J Comp Neurol 286:260–268.

Paxinos G, Watson C (1986) The rat brain in stereotaxic coordinates. San Diego: Academic.

Pfaff DW, Keiner M (1973) Atlas of estradiol-concentrating cells in the central nervous system of the female rat. J Comp Neurol 151:121–158.

Pfaff DW, Sakuma Y (1979a) Deficit in the lordosis reflex of female rats caused by lesions in the ventromedial nucleus of the hypothalamus. J Physiol (Lond) 288:203–210.

Pfaff DW, Sakuma Y (1979b) Facilitation of the lordosis reflex of female rats from the ventromedial nucleus of the hypothalamus. J Physiol (Lond) 288:189–202.

Pfaff DW, Schwartz-Giblin S, McCarthy MM, Kow L-M (1994) Cellular and molecular mechanisms of female reproductive behaviors. In: The

physiology of reproduction (Knobil E and Neill JD, eds), pp 107–220. New York: Raven.

Pfaus JG, Kleopoulos SP, Mobbs CV, Gibbs RB, Pfaff DW (1993) Sexual stimulation activates c-fos within estrogen-concentrating regions of the female rat forebrain. Brain Res 624:253–267.

Pilowksy PM, Lipski J, Prestidge R, Jiang C (1991) Dual fluorescence combined with a two-color immunoperoxidase technique: a new way of visualizing diverse neuronal elements. J Neurosci Methods 36:185–193.

Pleim ET, Brown TJ, MacLusky NJ, Etgen AM, Barfield RJ (1989) Dilute estradiol implants and progestin receptor induction in the ventromedial nucleus of the hypothalamus: correlation with receptive behavior in female rats. Endocrinology 124:1807–1812.

Polston EK, Erskine MS (1995) Patterns of induction of the immediate early genes c-fos and egr-1 in the female rat brain following differential amounts of mating stimulation. Neuroendocrinology 62:370–384.

Segarra AC, McEwen BS (1991) Estrogen increases spine density in ventromedial hypothalamic neurons of peripubertal rats. Neuroendocrinology 54:365–372.

Shugrue PJ, Bushnell CD, Dorsa DM (1992) Estrogen receptor messenger ribonucleic acid in female brain during the estrous cycle: a comparison with ovariectomized females and intact males. Endocrinology 131:381–388.

Simerly RB, Chang C, Muramatsu M, Swanson LW (1990) Distribution of androgen and estrogen receptor mRNA-containing cells in the rat brain: an in situ hybridization study. J Comp Neurol 294:76–95.

Swanson LW, Hartman BK (1975) The central adrenergic system. An immunofluorescence study of the location of cell bodies and their efferent connections in the rat utilizing dopamine beta hydroxylase as a marker. J Comp Neurol 163:467–506.

Szentagothai J, Flerko B, Mess B, Halasz B (1968) Hypothalmic control of the anterior pituitary. Budapest: Akademiai Kiado.

Tetel MJ, Getzinger MJ, Blaustein JD (1993) Fos expression in the rat brain following vaginal-cervical stimulation by mating and manual probing. J Neuroendocrinol 5:397–404.

van den Pol AN, Hermans-Borgmeyer I, Hofer M, Ghosh P, Heinemann S (1994) Ionotropic glutamate receptor gene expression in hypothalamus: localization of AMPA, kainate, and NMDA receptor RNA with in situ hybridization. J Comp Neurol 343:428–444.

van den Pol AN, Romano C, Ghosh P (1995) Metabotropic glutamate receptor mGluR5 subcellular distribution and developmental expression in hypothalamus. J Comp Neurol 362:134–150.

Woolley CS, McEwen BS (1994) Estradiol regulates hippocampal dendritic spine density via an *N*-methyl-D-aspartate receptor-dependent mechanism. J Neurosci 14:7680–7687.